RESEARCH PAPER

NUMERICAL HYDRODYNAMIC MODELLING AS A TOOL FOR RESEARCH AND USE OF TIDAL RIVERS

Evgeniya D. Panchenko[1,2*], Andrei M. Alabyan[2,1], Tatiana A. Fedorova[1]

[1] Water Problems Institute of RAS, Gubkina str., 3, 117971, Moscow, Russia

[2] Lomonosov Moscow State University, Leninskie Gory, 1, 119991, Moscow, Russia

***Corresponding author:** panchenko.zhe@gmail.com

Received: November 16th, 2023 / Accepted: December 12th, 2023 / Published: March 31st, 2024

https://DOI-10.24057/2071-9388-2023-3122

ABSTRACT. Tidal estuaries play a crucial role, serving as major hubs for economic activities while also contributing to the preservation of natural diversity and bioproductivity. In Russia, these estuaries are primarily located in remote regions of the European North and the Far East, making them vital for energy and transportation usage as they essentially form the 'cores' of territorial development along the Northern Sea Route.

To facilitate the development of energy and navigation infrastructure in tidal estuaries, as well as to plan and implement environmental protection measures, it is essential to have a comprehensive understanding of their hydrological regime. Unlike regular river flow, tidal estuaries exhibit more complex hydrodynamics, influenced by both river and marine factors. Due to the considerable challenges of conducting field hydrological studies in remote areas, numerical hydrodynamic modelling has emerged as a valuable method for obtaining information on the flow and water level regime in tidal estuaries. This paper presents an application of one-dimensional HEC-RAS and two-dimensional STREAM_2D CUDA numerical models to investigate the parameters of reverse currents in the hypertidal Syomzha estuary flowing into the Mezen Bay of the White Sea. The limitations and accuracy of the models are discussed, along with the potential for their improvement considering recent advancements in understanding the hydraulics of reverse currents.

KEYWORDS: tidal estuary, reverse current, energy potential, mathematical model, White Sea, Syomzha river

CITATION: E. D. Panchenko, A. M. Alabyan, T. A. Fedorova (2024). Numerical Hydrodynamic Modelling As A Tool For Research And Use Of Tidal Rivers. Geography, Environment, Sustainability, 1(17), 36-43
https://DOI-10.24057/2071-9388-2023-3122

ACKNOWLEDGEMENTS: The authors are grateful to the participants of fieldwork – N.A. Demidenko, M. Leummens, L. Leummens, A. Popryadukhin, E. Fingert.

The work was supported by Russian Science Foundation project №22-29-01184, https://rscf.ru/project/22-29-01184/.

Conflict of interests: The authors reported no potential conflict of interest.

INTRODUCTION

Estuaries have always been important to people as transport links between the sea and river, providing shelter for sailors, recreation opportunities, and resources for fishing and hunting. The flora and fauna of estuarine areas are incredibly diverse; fertile soils, flat terrain, and abundant freshwater resources offer excellent potential for agriculture. Hence it is no surprise that some of the world's most densely populated coastal areas are located near estuaries, and it is even more pronounced along the Russian Arctic coast, where all major cities and essential towns are situated at the mouths of large or small rivers. In addition, in the case of tidal estuaries, the problem of energy supply even to remote settlements can be successfully solved owing to the development of several innovative solutions for the use of tidal energy (Khare et al. 2019; Neill and Hashemi 2018). The modern designs of in-channel units that do not require the construction of dams and barrages make tidal power plants even more economical and environmentally friendly.

At the same time, settlements along estuarine shores are not without their challenges and can face specific hazards, such as storm-surge floods or brackish water intrusions into water intakes. Navigational conditions in estuarine aquatories, especially in tidal ones, can significantly differ from those in rivers and the open sea due to reverse tidal currents and unpredictable channel deformations caused by intensive sediment transport. Estuarine hydrodynamics play a crucial role in shaping these natural processes, influenced by river and marine characteristics.

Tidal estuaries exhibit the most complex hydrodynamic features, which are characterized by rapid variations of flow structures and properties during the tidal cycle. Although essential estuarine hydrodynamics is well explained with field surveys and conceptual mathematical descriptions (Mikhailov 1971; McDowell and O'Connor 1977; Savenije 2012; Hoitink and Jay 2016), collecting high-resolution spatial and temporal data along the entire estuary from the river mouth to the adjacent section of the tidal river reach is laborious, time-consuming, and expensive (Miskevich et.al. 2018b; Veerapaga 2019). In many cases, numerical models offer the most effective alternative for complicated field campaigns and comprehensive analyses of the hydrodynamic measurements (Abreu et.al. 2020; Matte et.al. 2017).

Worldwide, a large number of hydrodynamic models of estuaries have been developed both for various economic purposes and to address different scientific questions (Alabyan et.al. 2022). These estuarine models are used to study the interaction of river flow with tidal and surge waves, to forecast floods and other hazards (Zheng et.al. 2020; Lyddon et.al. 2018; Ward et.al. 2018), and to assess the impact of current and expected climate change on estuarine flow dynamics (Chen et.al. 2015; Iglesias et.al. 2022; Panchenko et.al. 2020b; Anh et.al. 2018). Some models are specifically developed for monitoring estuarine processes such as salt intrusion (Mills et.al. 2021; Chen et.al 2015; Veerapaga et.al. 2019) and sediment transport (Jiang et.al. 2013; Yin et.al. 2019; Rahbani 2015). Hydrodynamic modelling is also used to determine optimal locations for the construction of engineering structures, to study currents for tidal energy utilization (Rtimi et.al. 2021), and to ensure favorable conditions for navigation (Jouanneau et.al. 2013).

While these models often reproduce the general features of the hydrodynamic regime, there can be significant quantitative differences between the modelling results and actual flow parameter values. Every model simplifies reality and comes with its strengths and weaknesses. Therefore, modelling results have a wide range of uncertainties related to errors, calibration parameters, model assumptions, and approximations used for initial conditions and forcing characteristics (Iglesias et.al. 2022; Khanarmuei et.al. 2020). Sometimes it is difficult to understand the main factor affecting modelling quality. Part of the errors stem from inaccuracies in channel and floodplain topography and boundary conditions (Khanarmuei et.al. 2020; Matte et.al. 2017), which, in turn, are linked to the practical difficulties of carrying out fieldwork in large estuaries and obtaining the full set of field data necessary for model construction and calibration.

The model dimensioning (1D, 2D or 3D) is still problematic and questionable (Samarasinghe et.al. 2022; Veerapaga et.al. 2019), depending on the research purpose, the object size and geometry, and the availability and accuracy of field data. When the primary aim of a study is to analyze changes in the hydrodynamic characteristics along a small tidal river, and the length of the study area exceeds the river width by two orders or more, it is preferable to use one-dimensional (1D) models. Such models require significantly fewer measurement data and less computational power and time for calculations compared to two-dimensional (2D) and three-dimensional (3D) models. Moreover, in a small estuary, owing to its size and relatively simple morphology and bed topography, it is possible to obtain highly accurate field data, allowing us to assess the actual capabilities of hydrodynamic models and to analyze the factors contributing to modelling errors.

Previously, estuarine hydrodynamics of small tidal rivers was investigated using one-dimensional models in the White Sea region, where tidal wave heights can vary from less than 1 m in the Laya River (a Northern Dvina delta branch tributary) to 9 m in the Syomzha River (a Mezen estuary tributary) (Panchenko 2023). For the hypertidal Syomzha estuary, differences between measured and modeled values of high and low water levels, as well as flood and ebb water discharges, ranged from 10 to 20%, even with high-accuracy bathymetry and boundary data available (Panchenko and Alabyan 2022). Similar results were reported by(Mohammadian et.al. 2022) for a 3D model of a hypertidal estuary, where despite accurate boundary conditions based on in-situ measurements, the best water level calibration results were of the same order of inaccuracy. This was attributed to the fact that hypertidal estuaries are characterized by extremely high variations in tidal depths over ebb-flood cycles, caused by significant spatial flow variations and interactions of complex currents with bathymetric features.

Previous research on the large mesotidal Onega estuary (Panchenko et.al. 2020c), undertaken on the background of reliable field data, demonstrated good agreement of 1D model calculations with both results of the 2DH (depth-averaged 2D model) and measured values of water levels and flow parameters, only when focusing on averaged values across the cross-section. This research aims to compare 1D and 2DH modelling results for a very different environment – the small hypertidal estuary – where all hydrodynamic processes are much more rapid and pronounced throughout the tidal cycle. The Syomzha estuary was selected as the research object, with fieldwork held in the summer low water periods of 2015 and 2018 to ensure a sufficient dataset for model construction, calibration and validation (Panchenko et.al. 2020a; Panchenko and Alabyan 2022).

MATERIALS AND METHODS

The study area

The study object is the Syomzha estuary. The Syomzha River meets the Mezen estuary near its mouth (Fig.1, 2). The Syomzha is 63 km long and has a catchment area of 490 km^2. The average slope of the river is 0.61‰, and the average slope of the estuary bottom is three times less at 0.26‰. There are no gauging stations along the river, but estimates suggest that an average summer low-water river runoff is about 5 m^3/s, with a maximum spring snow-melt flood discharge of 5% probability reaching around 200 m^3/s, nearly equivalent to the maximum flood and ebb tidal flow at the river mouth during the low-water period. The tide in the White Sea is semidiurnal of regular sinusoidal shape in the open sea. At the Syomzha mouth, the spring tidal range exceeds 8.5 m, increasing relative to the open sea due to the confusor effect along the narrowing Mezen Bay and the Mezen estuary. Under summer low-water conditions, the tidal stretch of the river spans approximately 23–25 km, constituting roughly one-third of the total river length.

In lower cross-sections, the maximum flow depth fluctuates between 1 and 10 m, with the river bed primarily composed of loess and mud, while sand and gravel accumulative forms concentrate along the dynamic axis of the tidal currents. The tidal wave decreases in height upstream to approximately 5–6 m at 4 km and 3–4 m at 8 km.

The river channel is characterized by a meandering pattern. The width of the estuary changes significantly during the tidal cycle. At the mouth, it widens to 90 m at high water and contracts to 30 m at low water (Fig. 2). Further upstream, the range of river width and depth tidal oscillation declines, along with the corresponding decrease in tidal wave height. At 10 km upstream from the mouth, the channel width ranges from 20 to 30 m, and at 21 km, it narrows to 10–15 m regardless of the tidal cycle phase. The depth at low tide averages around 0.8 meters, dropping to 0.3–0.5 m at gravel ripples and rising to 1.5–2.0 m in pools.

The methodology

To explore the hydraulic regime of the Syomzha estuary and to gather the necessary data for numerical modelling, field campaigns were carried out in August

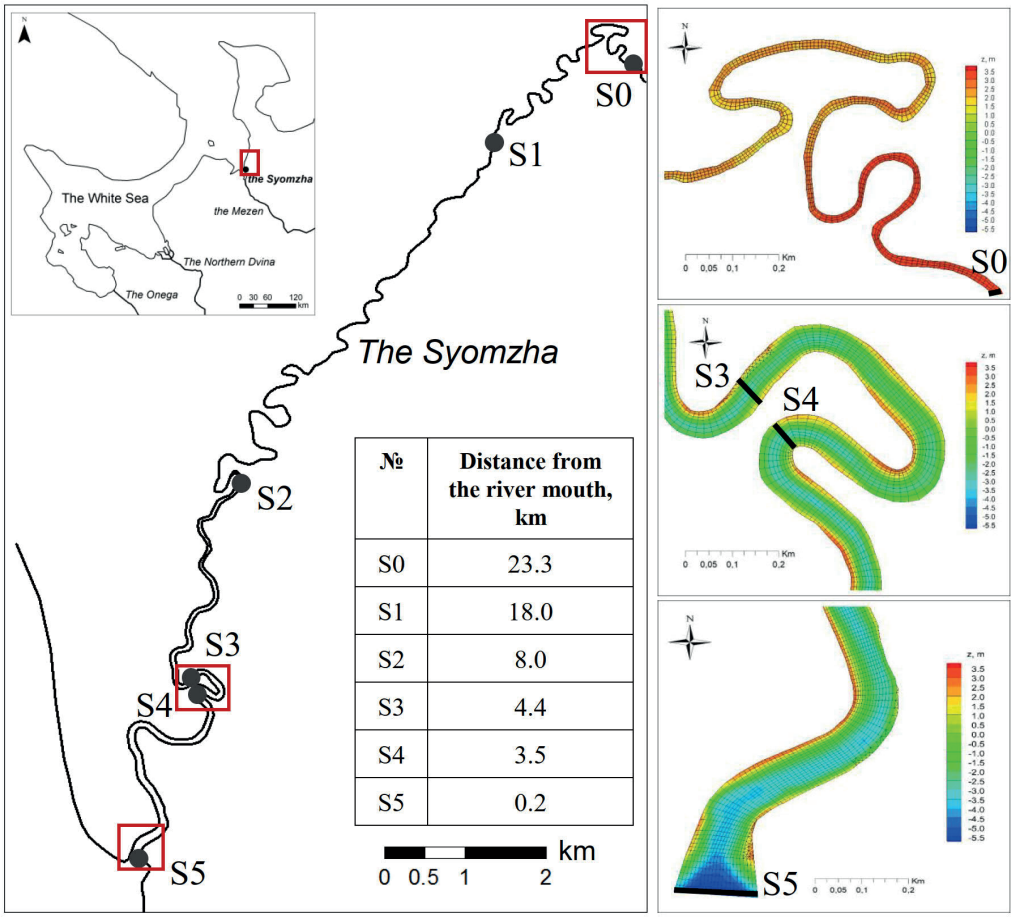

Fig. 1. Location of the study area and the Syomzha River section under modelling with enlarged fragments of key sections

Fig. 2. The Syomzha River mouth at (a) high and (b) low water

2015 and August 2018. These measurements took place during the summer low-flow period when the river runoff was around 5–7 m^3/s. In 2015, water levels were recorded by barometric loggers at points S1, S2, and S5 (Fig. 1), while flow measurements with an Acoustic Doppler Current Profiler (ADCP) were undertaken at S2, specifically during flood flow (not covering the full tidal cycle). Tidal water level oscillations were deemed negligible at point S0.

The 2018 surveys were more extensive: water levels were measured at five points (S1–S5) with the unified zero-mark, and runoff and flow velocity were measured with two ADCPs concurrently at cross-sections S3 and S4 throughout the entire tidal cycle (Panchenko et.al. 2020a; Panchenko and Alabyan 2022). Simultaneously, a bottom relief survey was undertaken together with an examination of brackish water intrusion from the Mezen estuary and its mixing with the freshwater of the Syomzha River.

The obtained data on the detailed channel bathymetry served as the foundation for the digital elevation model (DEM) used in both the 1D and 2DH hydrodynamic models. Non-stationary low boundary conditions for the models were formed based on records from a level logger located at the lowest point, S5. The upper boundary condition was a stationary inflow discharge of 7 m^3/s at point S0, located 23.5 km upstream from the mouth, where the flow dynamics is no longer affected by sea level tidal oscillations. The HEC-RAS software (Brunner 2016), solving the full one-dimensional Saint-Venant equations, was used for 1D modelling of the hydrodynamic regime of the Syomzha estuary. The geometry cross-sections in the 1D model were defined with a step of 100–150 m (147 cross-sections in total).

The 2DH model was developed using the STREAM 2D CUDA package, based on shallow water equations and their numerical solution for shallow water flows with shoaling areas and bottom discontinuities (Aleksyuk and

Belikov 2017a,b). The mesh of 2DH model consisted of 17,602 rectangular cells with varying sizes, ranging from 10 to 20 m in length and 5 m in width. The bottom bathymetry in both models was kept consistent.

The calibration of the 1D and 2D models was conducted for the hydrological situation during two tidal cycles of August 13–14, 2018. The only calibrating parameter for both models was the Manning's roughness coefficient. By adjusting its values along the river sections, the goal was to achieve the best model results compared to measured water levels and discharges. The data collected on August 6, 2015, were used to validate the models (model test on the independent dataset not used for the calibration routine).

RESULTS

Following the calibration routine of both models, the Syomzha River stretch covered by the modelling was divided into three zones with varying roughness coefficient values: 1) n = 0.015 up to 5 km from the mouth cross-section; 2) n = 0.02 between 5 and 10 km; 3) n = 0.03 upstream of 10 km. This division enabled the attainment of realistic results for all measurement sites in terms of both water level and flow oscillations during the tidal cycle (Fig.3, 4), as well as facilitated the termination of water level fluctuations at the upper boundary of the model.

Following the calibration, both the 1D and 2D models showed nearly identical results in terms of predicted water levels (Fig. 3). At the S4 location, the actual range of water level changes was 6.2 m, whereas in the 1D model, it was 5.8 m, and in the 2D model it was 5.7 m (with modeled ranges being 6–8% lower). At the same time, at the S4 location, where the measured tidal range was 3.72 m, the modeled value in both models was 3.12 m (15% less). At the S1 location, the measured range was 1.1 m, while the simulated ranges were 1.05 m and 0.9 m in the 1D and 2D models, respectively.

At S2, the minimum water levels before the tidal rise were modeled with high accuracy (2–5 cm difference), but the maximum water level in the models was lowered by more than 0.5 m (Fig. 3, b). The modeled maximum level nearly coincided with the maximum level set at the lower boundary. However, according to the measurement data from both expeditions, the maximum water level in this section exceeded the maximum at the lower boundary by about 0.8 m.

Conversely, ebb water levels were less accurately modeled at locations S3 and S4. At S4, ebb water levels in the models were overestimated relative to actual levels by 0.54 and 0.78 m (1D and 2D, respectively), while the maximum levels differed only by 0.18 m. Although the difference in tidal range did not exceed 15% at S4, the difference in minimum levels was significant and comparable with the low water depth at the cross-section (Fig. 3, a). Nonetheless, this inaccuracy is not of critical importance when analyzing the pattern of tidal wave propagation and transformation.

The timing of tidal peaks and troughs was reproduced quite accurately by both models, with a difference of no more than 10 minutes in all locations (which is comparable to the accuracy of visually registering the time of a current slowing down at the beginning of the tide). In other words, the tidal propagation velocity was modeled very accurately. At calibration points S3 and S4, changes in water discharges during the tidal cycle were closely reproduced by both models (Fig. 4), but the difference between 1D and 2D results increased with distance from the lower boundary. The ebb discharge during the tide was accurately computed by both models. For peak flood and ebb discharges, the difference between measured and modelled values at both locations did not exceed 30 m³/s, which was less than 10% of the discharge range.

The availability of measured water levels and discharges for another period during the summer of 2015 allowed for the validation of the selected roughness characteristics on

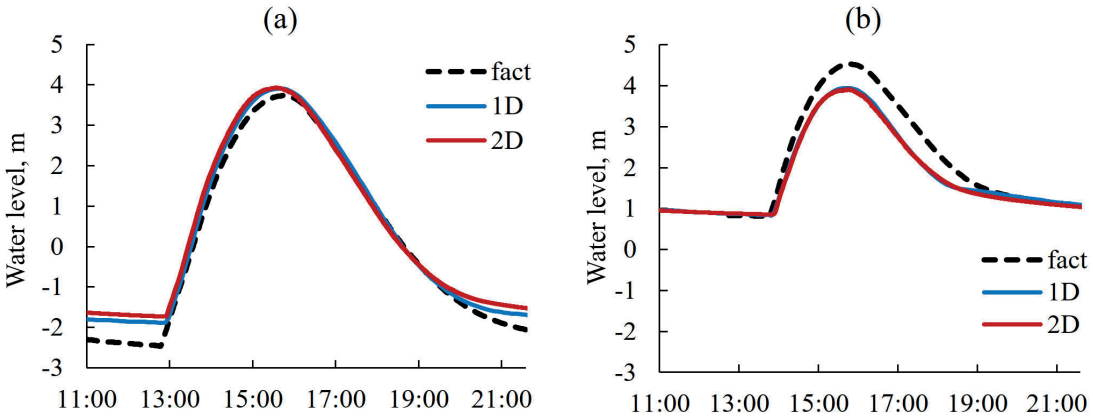

Fig. 3. Model calibration results: water levels at (a) the S4 location; (b) the S2 location on August 14, 2018

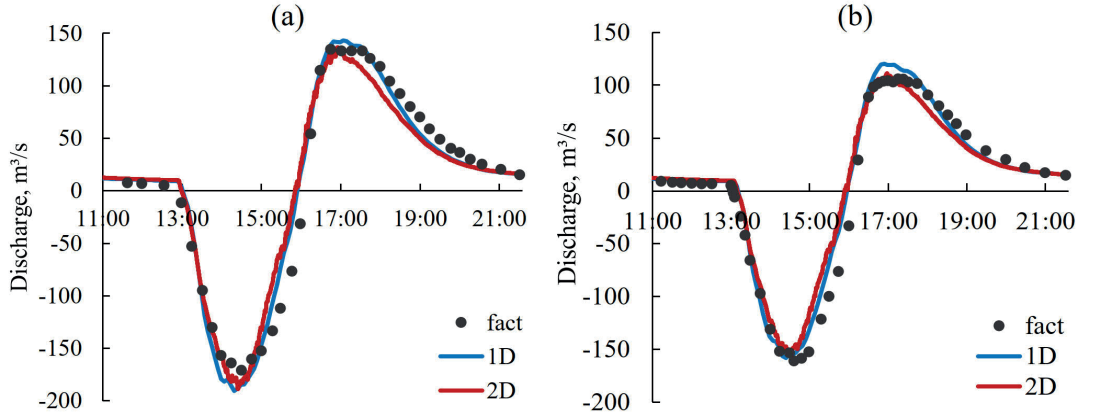

Fig. 4. Model calibration results: discharges at (a) the S4 location; (b) the S3 location on August 14, 2018

independent data. A pattern similar to what was observed during the calibration process can also be seen for the model validation.

At the S2 location, the measured tidal range was 3.07 m, and the simulated ranges were 2.43 m and 2.36 m in 1D and 2D, respectively (the modeled values were 20 – 23% lower) with the largest difference for the maximum level (Fig. 5). The times of the maximum flood tide discharge (negative value) and current reversal during tide at S2 were accurately predicted by both models. However, both models underestimated the value of the peak flood discharge: 46.6 m^3/s and 39.7 m^3/s for the 1D and 2D models, respectively, compared to the measured 56 m^3/s.

The slightly better results of the 1D model compared to the 2D one can be explained by the fact that the calibration was performed on the one-dimensional model, and the selected roughness values were used in both cases. If there were enough field data to calibrate the 2D model, this contradiction could be eliminated.

The tidal wave propagation celerity was 1.3 m/s between points S2 and S5 and 1.5 m/s between points S1 and S2, which corresponded to reality for both models.

Thus, we can assume that in cases where it is necessary to calculate flow characteristics averaged over the cross-section of the channel, the use of a one-dimensional model is preferable since it has an accuracy that is at least no less than that of a two-dimensional model and requires much less labor and machine time.

The use of a two-dimensional model provides an advantage when analyzing changes in the flow velocity spatial distribution during the tidal cycle. For instance, in Fig. 6, an example is presented of how, at the same water discharge of 100 m^3/s (in different directions), the flow concentrates along its dynamic axis as the tidal flood and ebb currents develop.

Such an analysis may be necessary when calculating the trajectories of sediment and pollutants, bed deformations, and projecting the location and design of water intakes and dispersing water outlets. Of particular interest is the velocity field of the slack water period when the water masses do not stand still, but form a complex system of large-scale eddies, constantly transforming and migrating across the water area (Fig. 7).

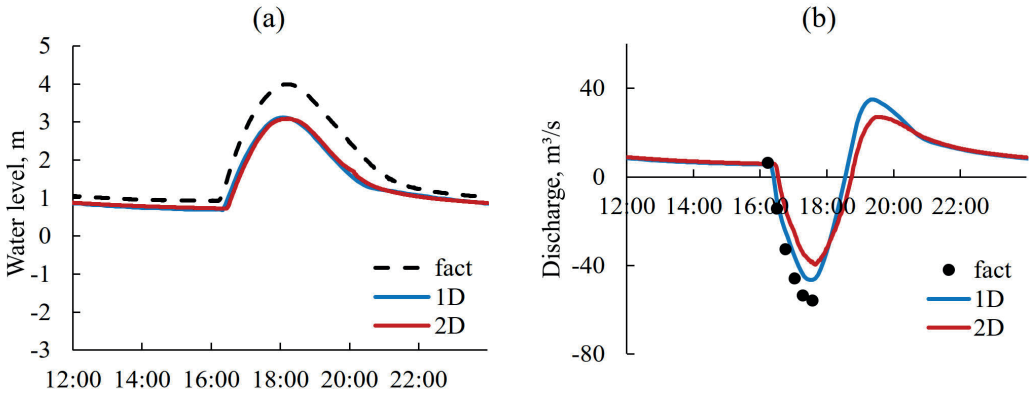

Fig. 5. Model validation results: (a) water levels and (b) discharges at the S2 location on August 6, 2015

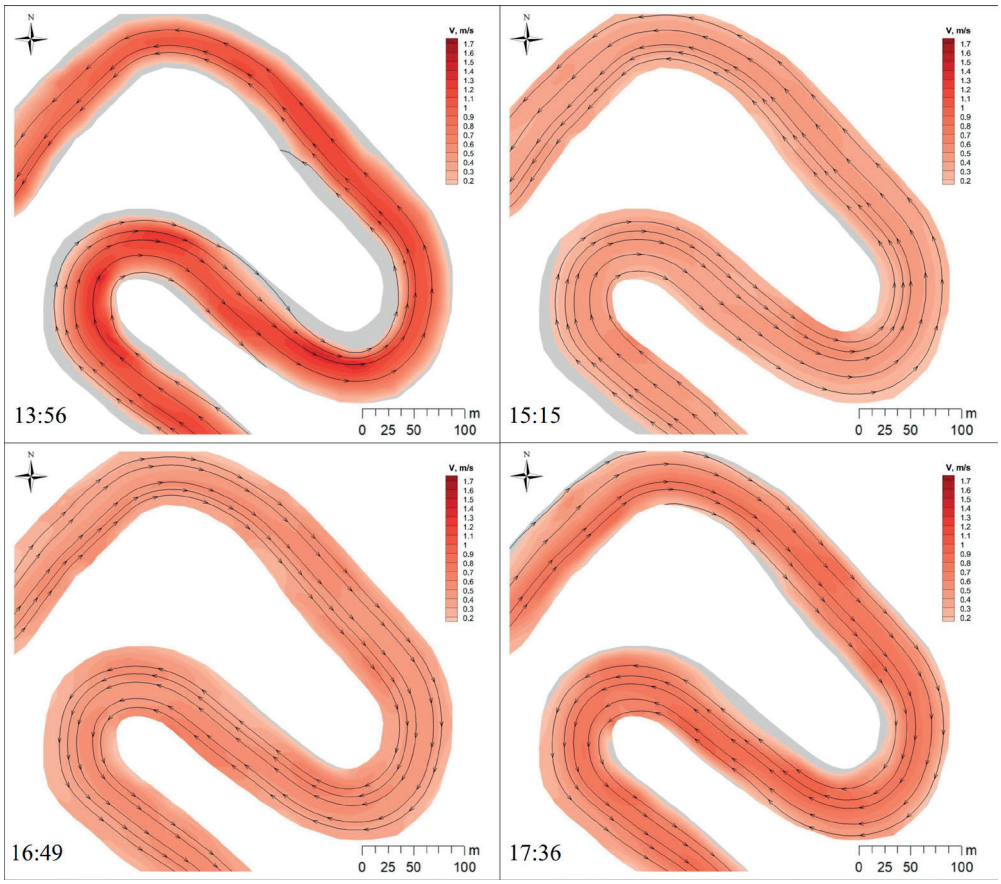

Fig. 6. 2D simulated flow velocity spatial distribution on August 14, 2018

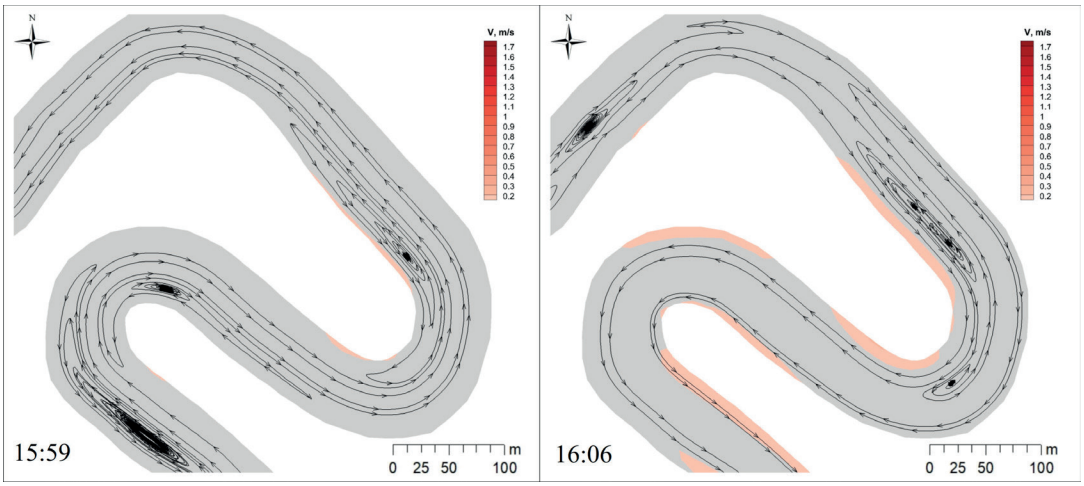

Fig. 7. 2D simulated flow velocity fields near slack water on August 14, 2018

DISCUSSION

The use of numerical hydrodynamic models to study the regime of the hypertidal Syomzha estuary made it possible, based on point hydrological measurements, to demonstrate a continuum picture of hydrodynamic processes throughout the full tidal cycle along the estuary. At the same time, the results of field measurements were used to calibrate and validate the models.

The transformation pattern of the tidal wave, as well as the order of occurrence of water level and flow peaks during the tidal cycle on the Syomzha, are quite consistent with the main patterns established on other tidal rivers during similar, but more detailed and lengthy field measurements (Miskevich et.al. 2018a, Panchenko et.al. 2020). The modelling inaccuracies may be associated both with the insufficient detail of the bottom relief pattern and with the underestimation of some features of the reverse flow hydraulics identified in recent studies (Panchenko and Alabyan 2022). The possibility of taking into account changeable hydraulic resistance and eddy viscosity when modelling may represent a way to improve the reverse flow simulation results. Since the river runoff in August 2018 was comparable to the inaccuracy in tidal flow modelling, its influence can be considered insignificant, at least for the summer low-water period.

On a tidal estuary, during semidiurnal tides during low water, the direction of the river flow changes four times a day. In this case, the values of maximum water flow rates at high and low tides can be quite comparable with the flow rate of spring floods caused by snowmelt. Unlike snowmelt and rain floods, tidal floods repeat with a certain periodicity, determined solely by astronomical factors. Their predictability is an important positive aspect when planning and carrying out activities related to ensuring safe navigation and fishing, the operation of water intakes and dispersing water outlets, as well as other activities related to the sustainable use of water resources. Since tides are more predictable than the wind and the sun, tidal power is considered to be the most preferable renewable energy source in the environment of the Russian Arctic and Far East. Even on such a small river as the Syomzha, a chain of in-channel units, switched on as the tidal wave passes, can provide a stable energy supply to the surrounding area.

CONCLUSIONS

Both one-dimensional and two-dimensional models can be successfully used to study the regime of tidal rivers: determining the tidal wave celerity and transformation when propagating upstream, the time of high and low water, and the moment of slack water and current reversal; maximum tidal flood and ebb flow at different distances from the river mouth are less accurately reproduced, but with an acceptable accuracy of about 20%. The advantage of a one-dimensional model is that it requires less labor to prepare the initial data and significantly reduces computer calculation time. The use of two-dimensional models is necessary in cases where the research object is not only the flow parameters averaged over the cross-section but also their distribution over the channel width and the aquatory as a whole. A necessary condition for the use of numerical hydrodynamic modelling to solve engineering and environmental issues is their calibration and validation based on reliable field data.

REFERENCES

Abreu C., Barros M., Brito D., Teixeira M., Cunha A. (2020). Hydrodynamic Modeling and Simulation of Water Residence Time in the Estuary of the Lower Amazon River. Water, 12(3), 660, DOI:10.3390/w12030660.

Alabyan A., Panchenko E., Alekseeva A. (2018). Hydrodynamic features of small tidal estuaries of the White Sea basin // Vestnik Moskovskogo Universiteta, Seria 5 Geographia, 4, 39–48. (in Russian with English summary).

Alabyan A., Krylenko I., Lebedeva S., Panchenko E. (2022). World experience in numerical simulation of flow dynamics at river mouths. Water Resources, 49 (5), 766–780. DOI: 10.1134/S0097807822050025.

Aleksyuk A., Belikov V. (2017). Simulation of shallow water flows with shoaling areas and bottom discontinuities. Computational Mathematics and Mathematical Physics, 57 (2), 318–339, DOI: 10.1134/S0965542517020026.

Aleksyuk A., Belikov V. (2017). STREAM 2D CUDA program complex for calculation of currents, bottom deformations and pollution transport in open streams using CUDA technology (on NVIDIA GPUs). Software Registration Certificate No. 2017660266. (in Russian).

Anh D., Hoang L., Bui M., Rutschmann P. (2018). Simulating Future Flows and Salinity Intrusion Using Combined One- and Two-Dimensional Hydrodynamic Modelling—The Case of Hau River, Vietnamese Mekong Delta. Water, 10(7), 897, DOI:10.3390/w10070897.

Brunner G. (2016). HEC-RAS River Analysis System User's Manual. Version 5.0. US Army Corps of Engineers, Institute for Water Resources, Hydrologic Engineering Center, Davis, CA, USA. 960 p.

Chen W., Chen K., Kuang C., Zhu D., He L., Mao X., Liang H., Song H. (2016). Influence of sea level rise on saline water intrusion in the Yangtze River Estuary, China. Applied Ocean Research, 54, 12–25, DOI: 10.1016/j.apor.2015.11.002.

Hoitink A., Jay D. (2016). Tidal river dynamics: Implications for deltas. Rev. Geophys., 54, 240–272, DOI:10.1002/2015RG000507.

Iglesias I., Bio A., Melo W., Avilez-Valente P., Pinho J., Cruz M., Gomes A., Vieira J., Bastos L., Veloso-Gomes F. (2022). Hydrodynamic Model Ensembles for Climate Change Projections in Estuarine Regions. Water, 14, 1966, DOI: 10.3390/w14121966.

Jiang A., Ranasinghe R., Cowell P. (2013). Contemporary hydrodynamics and morphological change of a microtidal estuary: a numerical modelling study. Ocean Dynamics, 63(1), 21–41, DOI:10.1007/s10236-012-0583-z.

Jouanneau N., Sentchev A., Dumas F. (2013). Numerical modelling of circulation and dispersion processes in Boulogne-sur-Mer harbour (Eastern English Channel): Sensitivity to physical forcing and harbour design. Deutsche Hydrographische Zeitschrift, 63 (11–12), 321–1340, DOI:10.1007/s10236-013-0659-4.

Khanarmuei M., Suara K., Sumihar J., Brown R.J. (2020). Hydrodynamic modelling and model sensitivities to bed roughness and bathymetry offset in a micro-tidal estuary. Journal of Hydroinformatics, 22 (6), 1536–1553, DOI:10.2166/hydro.2020.102.

Khare V., Khare C., Nema S., Baredar P. (2019). Tidal Energy Systems. Design, Optimization and Control. Elsevier. DOI: 10.1016/C2017-0-02279-6.

Lyddon C., Brown J., Leonardi N., Plater A. (2018). Flood Hazard Assessment for a Hyper-Tidal Estuary as a Function of Tide-Surge-Morphology Interaction. Estuaries and Coasts, 41, 1565–1586, DOI:10.1007/s12237-018-0384-9.

Matte, P., Secretan, Y., Morin, J. (2017). Hydrodynamic modeling of the St. Lawrence fluvial estuary. I: model setup, calibration, and validation. Journal of Waterway, Port, Coastal, and Ocean Engineering, 143 (5), DOI:10.1061/(ASCE)WW.1943-5460.0000397.

Miskevich I., Alabyan A., Korobov V., Demidenko N., Popryadukhin A. (2018). Short-term variability of hydrological and hydrochemical characteristics of the Kyanda estuary in Onega bay, the White sea (July 28–August 15). Oceanology, 58(3), 350–353, DOI: 10.1134/S000143701803013X.

Miskevich I., Korobov V., Alabyan A. (2018). Specificity of engineering-ecological surveys in small tidal estuaries of the western sector of the Russian Arctic. Engineering Survey, 12 (3-4), 50–61, DOI: 10.25296/1997-8650-2018-12-3-4-50-61(in Russian with English summary)

McDowell D., O'Connor B. (1977). Hydraulic behavior of estuaries. London: Macmillan Press.

Mikhailov V. (1971). Flow and channel dynamics in non-tidal river mouths. Moscow: Gidrometeoizdat. (in Russian)

Mills L., Janeiro J., Martins F. (2021). Effects of sea level rise on salinity and tidal flooding patterns in the Guadiana Estuary. Journal of Water and Climate Change, 12 (7), 2933–2947, DOI: 10.2166/wcc.2021.202.

Mohammadian A., Morse B., Robert J.-L. (2022). Calibration of a 3D hydrodynamic model for a hypertidal estuary with complex irregular bathymetry using adaptive parametrization of bottom roughness and eddy viscosity. Estuarine, Coastal and Shelf Science, 265, 107655, DOI: 10.1016/j.ecss.2021.107655.

Neill S., Reza Hashemi M. (2018). Fundamentals of Ocean Renewable Energy: Generating Electricity from the Sea. London: Academic Press. DOI: 10.1016/C2016-0-00230-9.

Panchenko E., Alabyan A., Demidenko N., Leummens M., Leummens L. (2020). Data from the research on hydrodynamic characteristics of the macrotidal estuary of the Semzha River (White Sea basin). Version 1, 4TU.ResearchData, dataset. DOI:10.4121/uuid:890d12be-ddc9-42dc-a889-752783670136.

Panchenko E., Alabyan A., Krylenko I., Lebedeva S. (2020). Modelling of hydrodynamic processes in the Onega and the Northern Dvina river mouths under different climate change scenarios. Proc. IX International Scientific and Practical Conference «Marine Research and Education (MARESEDU-2020)», 2, 72–75. (in Russian)

Panchenko E., Leummens M., Lebedeva S. (2020). Hydrodynamic modelling of the Onega river tidal estuary. E3S Web Conferences, 163, DOI: 10.1051/e3sconf/202016301008.

Panchenko E., Alabyan A. (2022). Friction factor evaluation in tidal rivers and estuaries. METHODSX, 9, 101669, DOI:10.1016/j.mex.2022.101669.

Panchenko E. (2023). Experience of one-dimensional hydrodynamic modeling in micro-, meso- and macrotidal estuaries of small rivers. Collection of articles on the materials of the XIII seminar of young scientists of universities, united by the council on the problem of erosion, channel and estuarine processes. Moscow: Your format. 94–100. (in Russian).

Rahbani M. (2015). A comparison between the suspended sediment concentrations derived from DELFT3D model and collected using transmissometer – a case study in tidally dominated area of Dithmarschen Bight. Oceanologia, 57, 44–49, DOI:10.1016/j.oceano.2014.06.002.

Rtimi R., Sottolichio A., Tassi P. (2021). Hydrodynamics of a hyper-tidal estuary influenced by the world's second largest tidal power station (Rance estuary, France). Estuarine, Coastal and Shelf Science, 250, 19, DOI: 10.1016/j.ecss.2020.107143.

Samarasinghe J., Basnayaka V., Gunathilake M., Azamathulla H., Rathnayake U. (2022). Comparing Combined 1D/2D and 2D Hydraulic Simulations Using High-Resolution Topographic Data: Examples from Sri Lanka—Lower Kelani River Basin. Hydrology, 9 (2), 39, DOI: 10.3390/hydrology9020039.

Savenije H. (2012). Salinity and tides in alluvial estuaries. 2nd completely revised ed. Delft: Delft University of Technology.

Veerapaga N., Azhikodan G., Shintani T., Iwamoto N., Yokoyama K. (2019). A three-dimensional environmental hydrodynamic model, Fantom-Refined: Validation and application for saltwater intrusion in a meso-macrotidal estuary. Ocean Modelling, 141, DOI: 10.1016/j.ocemod.2019.101425.

Ward, P., Couasnon A., Eilander D., Haigh I., Hendry A., Muis S., Veldkamp T., Winsemius H., Wahl T. (2018). Dependence between high sea-level and high river discharge increases flood hazard in global deltas and estuaries. Environ. Res. Lett. 13, 084012, DOI: 10.1088/1748-9326/aad400.

Yin Y., Karunarathna H., Reeve D. (2019). Numerical modelling of hydrodynamic and morphodynamic response of a meso-tidal estuary inlet to the impacts of global climate variabilities. Marine Geology, 407, 229–247, DOI: 10.1016/j.margeo.2018.11.005.

Zheng P., Li M., Wang C., Wolf J., Chen X., De Dominicis M., Yao P., Hu Z. (2020). Tide-Surge Interaction in the Pearl River Estuary: A Case Study of Typhoon Hato. Frontiers in Marine Science, 7, DOI:10.3389/fmars.2020.00236.